1960

# $^1$H NMR relaxation study of paper as a system of cellulose and water

DONATELLA CAPITANI, ANNA LAURA SEGRE, DONATO ATTANASIO, BARBARA BLICHARSKA, BONAVENTURA FOCHER, AND GIORGIO CAPRETTI

**ABSTRACT**

*The interaction between water and cellulose was studied in papers sized with neutral alkylketene dimer and in papers prepared with acidic rosin sizing. We analyzed samples using nuclear magnetic resonance (NMR) and electron paramagnetic resonance (EPR). We measured molar ratios of cellulose/total water and cellulose/bound water. For linter and kraft acid papers, bound water is lower in acidic papers than in their neutral counterparts. The water content in groundwood paper is almost twice that of linter and kraft papers.*

ANALYSIS BY NUCLEAR MAGNETIC resonance (NMR) techniques has provided information on both the macromolecular structure and the dynamics of cellulose *(1, 2)*. High-resolution spectra of cellulose have allowed researchers to observe the fundamental polymorphism in cellulose and to characterize two different types of the native crystalline cellulose *(3, 4)*. These results have been confirmed by electron diffraction experiments on micro-crystals, leading to partially resolved structures *(5)*.

In cellulose samples of different origins, the proportions of crystalline polymorphs and other forms can be completely different. Moreover, amorphous fractions may be also present *(6, 7)*. $^1$H NMR relaxation techniques have been used to distinguish between crystalline and paracrystalline domains of cellulose microfibrils *(8)*. Results are in agreement with the observation that a lower packing density characterizes paracrystalline cellulose domains.

In previous work, we characterized some important features of an antique paper dating back to the 15th century *(7)*. We viewed the paper as a two-component material made of cellulose and water. Our analytical approach combined the echniques of pulsed low-resolution NMR, electron paramagnetic resonance (EPR) *(9, 10)*, and $^{13}$C CP-MAS cross polarization–magnetic angle pinning). This approach allowed us o characterize some of the chemical transformations that take place in the degradation of antique paper.

In our research work on the structure of recently made papers, we have focused mostly on the water–cellulose interactions, with attention to cellulose packing. We carried out experiments using pulsed $^1$H NMR relaxation to study the bound water and free water in cellulose. Because paramagnetic impurities play a role in the NMR relaxation process, we also performed spectroscopy experiments using EPR.

## EXPERIMENTAL PROCEDURES

### *Preparation of handsheets*

The commercial pulps used to make the handsheets were bleached pine kraft pulp, cotton linters (or rag stock), and groundwood spruce pulp. Kraft and linters pulps were soaked in water and beaten in a Valley beater to Schopper-Riegler freenesses of 28°SR and 30°SR, respectively. Groundwood pulp, with a freeness of 55°SR, was used as received.

Handsheet papers were prepared with neutral sizing and with acidic rosin sizing. Commercial alkylketene dimer (AKD) was used in neutral sizing. The synthetic size was added to the fiber stock at pH 8.0 at 0.6% consistency (1.3% on o.d. pulp), with the pulp containing calcium carbonate filler (10% on a.d. pulp). Handsheets were prepared in the laboratory according to TAPPI Test Method T 205. These papers were air dried and heated for 10 min at 105°C.

For handsheets prepared with acidic sizing, commercial rosin size was added to the fiber suspension (2.5% on o.d. pulp). The pH was corrected to pH 5.0 using $H_2SO_4$ and alum. Kaolin was finally added (8.3% on o.d. pulp). Handsheets were prepared according to TAPPI T 205 and were air dried and heated for 10 min at 105°C.

The degree of sizing was measured according to the Cobb$_{60}$ test method (TAPPI T 441). For paper sized with AKD and those sized with rosin sizing, respectively, the results were:

- Kraft: 25.0 and 23.4 g/m$^2$
- Linters: 30.0 and 28.0 g/m$^2$
- Groundwood: 17.5 and 12.7 g/m$^2$.

### *Electron paramagnetic resonance*

Electron paramagnetic resonance spectra were recorded at the X-band frequency (about 9.1 GHz) and at about 100 K, for a better signal-to-noise ratio, using a Varian E-9 spectrometer equipped with a standard variable temperature accessory. The field was measured with a Bruker BNM-20 gaussmeter, and the frequency was measured with a Systron-Donner 6246A counter. All samples were of comparable weight (about 30 mg). Sample heights were kept within 5 mm, so as to be well contained within the maximum sensitivity region of the instrument cavity.

Ion concentrations were determined only in the case of rhombic iron by comparing the signal areas with appropriate calibration curves *(10)*. Frozen solutions of $Fe(C_4H_6N_2)_3Cl_3$ (in which $C_4H_6N_2$ is 3-methylpyrazole) in acetonitrile were used for calibration *(11)*. Measurements made with control samples indicated that the total error was below 10%.

### *Nuclear magnetic resonance*

Samples of paper, stored at controlled conditions (23°C, 50% RH), were introduced into 5-mm NMR tubes, which were sealed. To keep the paper samples well within the NMR receiver coil, the height of each sample was approximately 0.5 cm. Each sample weighed 25.0 mg.

Free induction decays (FID) were acquired with a scan size of 2K words. The 90° pulse was 3.8 µs, and the dead time of the instrument was 8 µs. To get a good signal-to-noise ratio, we ran 16 scans.

Spin–lattice relaxation times, $T_1$, in the full temperature range, were measured with the aperiodic saturation recovery sequence. This sequence consists of a long train of 90° pulses (15 in our case) spaced out in an aperiodic way (by decreasing the interval linearly). The last, smallest spacing between two 90° pulses in the pulse train was 0.2 ms. At the end of the pulse train, the relaxation recovery starts and proceeds through the usual delay τ *(12)*.

The aperiodic saturation recovery sequence was run according to a multiblock, multiscan procedure. In each experiment, we collected either 64 or 256 blocks, corresponding to 64 and 256 different delays. In the temperature range of 293–233 K, each block was acquired with a time domain corresponding to a word size of 512. At lower temperature, when bound water is frozen and its long decay is no longer observable, a scan size of 64 words was used, which was enough for recording the

| | LINTERS | | KRAFT | | GROUNDWOOD | | |
|---|---|---|---|---|---|---|---|
| Temp., K | Neutral | Acidic | Neutral | Acidic | Neutral | Acidic | Ancient paper |
| 293 | 1.55±0.05 | 1.30±0.04 | 1.25±0.04 | 1.14±0.03 | 1.07±0.03 | 1.25±0.03 | 0.60±0.02 |
| 283 | 1.15±0.03 | 1.00±0.03 | 0.80±0.03 | 0.60±0.03 | 0.70±0.02 | 0.83±0.03 | 0.46±0.02 |
| 263 | 0.65±0.03 | 0.63±0.03 | 0.42±0.02 | 0.50±0.05 | 0.34±0.02 | 0.40±0.03 | 0.28±0.02 |

*I. $T_2$ spin–spin relaxation times for the slow relaxing component of water, milliseconds*

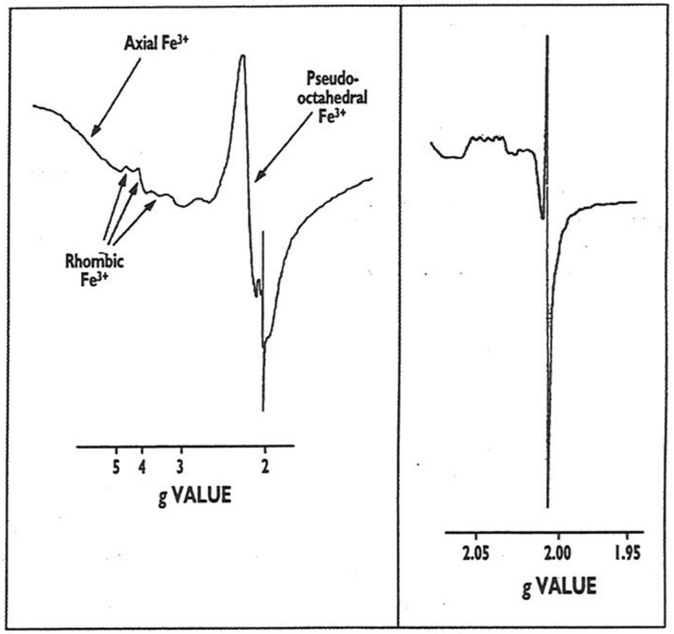

*I. The low-temperature (110 K), X-band EPR spectrum of an acid-sized linters sample (left). On the right is a magnification of the sharp radical line at g = 2.0035.*

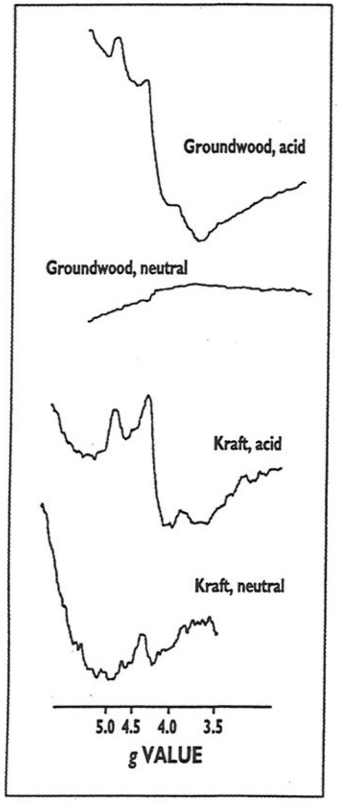

**2. Detail of the g = 4.3 region of 110 K, X-band EPR spectra for samples of groundwood pulp and kraft paper. The large difference in rhombic Fe$^{3+}$ content between the acid and neutral samples turns out clearly. The splitting of the signal into three absorptions indicates that the symmetry of iron slightly deviates from purely rhombic.**

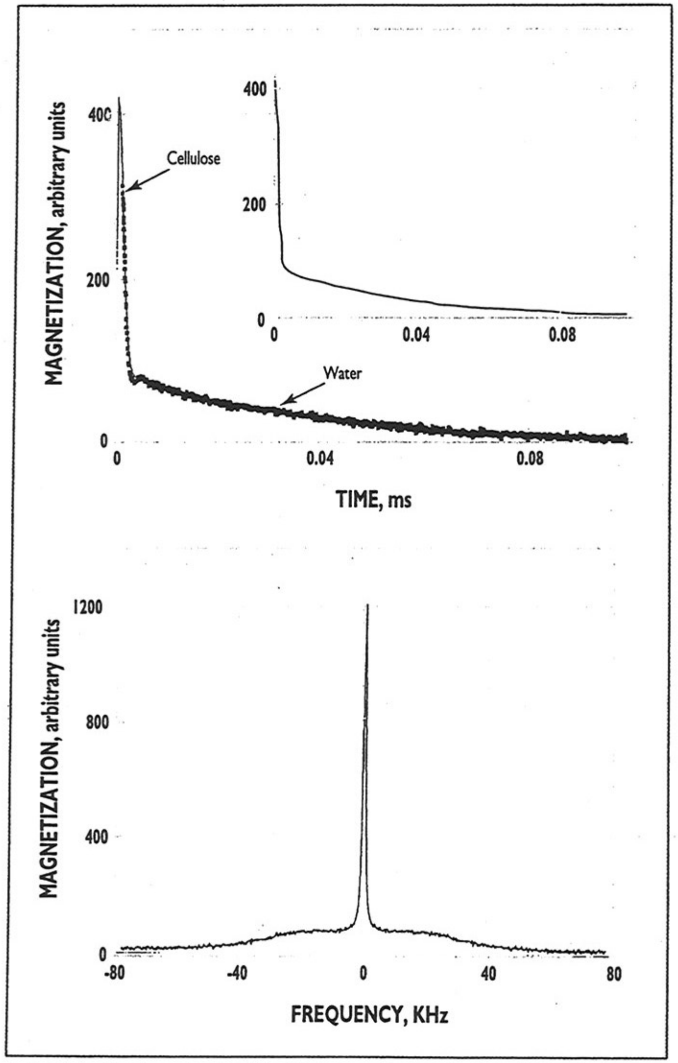

**3. Free induction decay (top) and its Fourier-transformed spectrum (bottom) of an untreated paper sample. A fully simulated FID is shown in the insert (13). Its Fourier-transformed spectrum is shown in the lower graph. (Temp. = 293 K. Spectrometer frequency = 57 MHz).**

fast decay of the cellulose and of the frozen water. To improve the signal-to-noise ratio, we allowed 16, 32, or 64 scans in the multiblock procedure.

The $T_2$ spin-spin measurements on the water component were carried out using a standard CPMG echo sequence, with $\tau/2$ = 20 µs. At least 512 echoes were collected *(13)*. The relative amount of total water in each sample was measured with a standard high-resolution spectrometer operating at 200 MHz (Bruker AC200), according to a procedure described previously *(7)*, at 298 K. All measurements were performed

| Temp., K | LINTERS |  | KRAFT |  | GROUNDWOOD[a] |  |  |
|---|---|---|---|---|---|---|---|
|  | Neutral | Sizing | Neutral | Sizing | Neutral | Sizing | Ancient paper[b] |
| 293 | 0.92 | 0.90 | 1.1 | 1.0 | 1.68 | 1.65 | 0.93 |
| 283 | 0.92 | 0.82 | 1.0 | 0.8 | 1.60 | 1.65 | 0.93 |
| 263 | 0.84 | 0.68 | 0.85 | 0.67 | 1.42 | 1.44 | 0.85 |

[a] Lignin not included. See the experimental section.
[b] Sample 1 from Ref. 7.
Errors are less than 5%.

**II. Molar ratios of [water]/[cellulose] at different temperatures. The difference in ratios between high temperature and low temperature gives the amount of free water.**

from high to low temperature. Whenever it was necessary to repeat a measurement, a fresh sample was prepared.

## ANALYSIS OF NMR DATA

We obtained the molar ratio between water and cellulose by analyzing the free induction decays in the time domain (2K data points). The FID shape was fit using the proper function. This function is the sum of a gaussian function, corresponding to the cellulose decay, and an exponential function, corresponding to the water decay:

$$Y = C_0 + [W_{cell}\exp(-G_{cell}\cdot t^2)] + [W_{water}\exp(-E_{water}\cdot t)] \quad (1)$$

where

$C_0$ = mean value of experimental noise
$W_{cell}$ = relative weight of the cellulose component
$W_{water}$ = relative weight of the water component
$G_{cell}$ = width of the gaussian decay
$E_{water}$ = width of the exponential decay.

All of the parameters are obtained from a best fit of the FID.

Solving Eq. 2 yields the molar ratio, *MR*, between water and cellulose:

$$MR = (W_{water}/n)\,/\,(W_{cell}/m) \quad (2)$$

where

$n$ = 2, the number of protons in the water
$m$ = 10, the number of protons in the monomeric unit of cellulose.

In groundwood pulp samples, a lignin content of 28% was subtracted from the total broad-band cellulose component. (We considered 10 protons to be a reasonable average per monomeric unit.) Since hemicelluloses in groundwood paper are mostly galactomannans, they have the same number of protons per monomeric unit of cellulose and do not need a separate treatment.

To calculate the relaxation times attributable to both the cellulose and the water, we treated the experimental data in the following way. In each block, resulting from the multiblock aperiodic saturation recovery sequence, we obtained the average value $Y_i$ of the first 20 points of the decay. These points are the actual values of the magnetization in the time range of 9–22 µs. In other words, $Y_i$ has been reported as a function of the value of the current block.

Through a best-fit procedure *(14)*, it is possible to obtain the relaxation times $T_i$ of the cellulose, introducing these average data in the multi-exponential function:

$$Y_i = \sum W_i \exp(-\tau / T_{li}) + C_0 \quad (3)$$

for $i$ = 1, …, $k$, where $k$ is the number of components. Here, $W_i$ represents the relative weight for each component.

With the same function, it is possible to obtain the relaxation times attributable to the water. To obtain relaxation times of the water, we introduce the mean value $Y_i$ of the points corresponding to the range 60–128 µs and apply a best-fit procedure again.

Cellulose and water have very different $T_2$ values. For the fast-relaxing cellulose component, $T_2$ is of the order of some tenth of a microsecond at room temperature. For the slowly relaxing water component, $T_2$ is of the order of 1 ms (Table I). As a result of these very different $T_2$ values, the cellulose component is fully decayed when the water component decay is measured. Therefore, under these conditions, it is possible to obtain the $T_{1,i}$ values of the cellulose and the $T_{1,i}$ values of the water.

As shown in **Table II**, the ratio of free water to bound water has been obtained by direct comparison of the FIDs at 10°C and -10°C. In fact, at low temperature, free water is frozen, with a large line width corresponding to a short decaying FID, while bound water is still quite mobile.

## RESULTS AND DISCUSSION

### *Study of EPR spectra*

**Figure 1** shows a representative EPR spectrum. The most evident characteristics are:

- A sharp radical line ($g = 2.0035$ and $\Delta\omega < 2$ gauss) of low and almost constant intensity
- An extremely broad signal (1400 -1700 gauss) centered at $g \approx 6$, for which the intensity depends strongly on the sample. (The variable g is essentially the ratio between the frequency and the magnetic field at which the resonance occurs, while $\Delta\omega$ is the line width expressed in gauss.)

Both of the above features were absent in the spectra of the antique paper made of rags. In the case of the groundwood pulp samples, the former signal at $g = 2.0035$ may be due to organic free radicals produced by the photolysis of lignin. Lignin is an aromatic polymer that can undergo different photochemical processes and produce phenoxyl radicals *(15)*.

Degraded samples of groundwood pulp paper often show intense and complex spectral patterns. These patterns should give us insights on the aging process. The origins of the radical lines in the kraft and linters samples, which do not contain lignin, are more puzzling. Since cellulose cannot be responsible for these radicals, we tentatively assume that they derive from the bleaching reagents used.

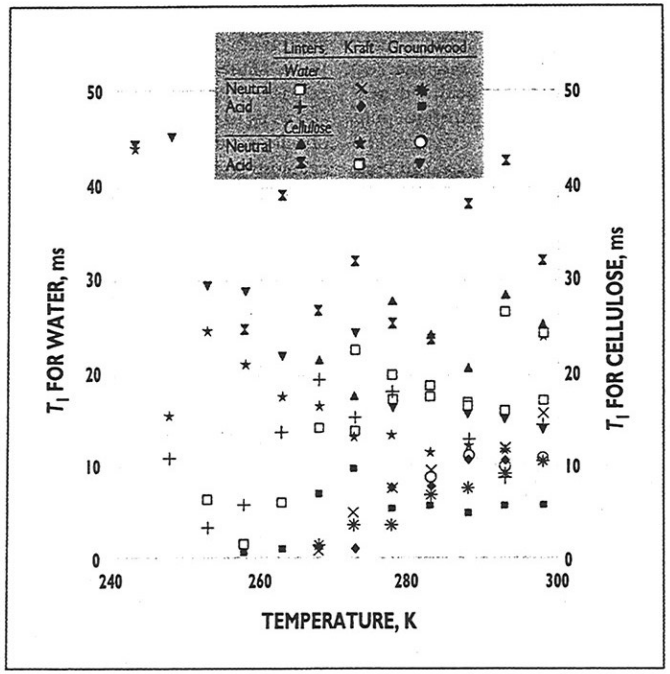

*4. Data on fast relaxing components of $T_1$ for water and $T_1$ for cellulose vs. temperature. No correlation can be discerned between these fast relaxation components.*

The broad signal at $g \approx 6$ is easily ascribed to high-spin $Fe^{3+}$ in a strongly distorted field of axial symmetry. This signal is capable of giving rise to large zero field splitting parameters *(16)*. Only transitions within the lowest Kramers' doublet are seen in this case, with a fictional spin 1/2 having $g_{\text{parallel}} = 2$ and $g_{\text{perpendicular}} = 6$, even though the real spin value remains 5/2 and the real $g$ value remains 2.0.

The observed spectrum is the perpendicular part of the signal, whereas the parallel absorption is too weak and broad to be detected. Similar spectra, exhibited by well-defined metallo-organic or biological molecules, are generally much sharper, with widths of a few hundred gauss. This observation suggests that the environment of iron in paper is much less defined and is spread over a wide interval of slightly different geometries. Furthermore, additional signals of variable but generally low intensity have been detected. These signals may be associated with traces of $Mn^{2+}$ and small amounts of $Fe^{3+}$ in quasi-octahedral ($g = 2.0$) or almost rhombic ($g \approx 4.3$) environments.

The most important paramagnetic impurity, $Fe^{3+}$, is present in these paper samples in three different stereochemical environments. One of these, the axial one, is dominant. However, while the amounts of both axial and octahedral iron are random and cannot be correlated with sizing or the type of paper, the rhombic species has been found

almost exclusively in the acid-sized samples. The spectra in **Fig. 2** show the large difference in rhombic $Fe^{3+}$ content between the acid and neutral samples for groundwood pulp and kraft papers. The experimental average concentrations are 100 ppm and 20 ppm, respectively, for the acid and neutral samples.

These paramagnetic impurities may act as strong relaxing agents. As a result, they may support the complex behavior of spin-lattice relaxation obtained by NMR (described below). In particular, rhombic iron at low temperature measurably shortens the $T_1$ relaxation of acid samples, in spite of its low concentration. Besides its efficiency as a spin relaxing agent, rhombic iron is also unique in favoring the hydrolytic degradation of cellulose *(10)*. A possible rationale for these findings is that iron attains this particular stereochemistry by binding directly to the cellulose backbone.

### *$^1$H NMR relaxation study*

As the upper graph of **Fig. 3** shows, the free induction decay of a sheet of paper is marked by two distinct parts. The first part is a rapid decay attributed to the decay of cellulose. The second part is much slower and is attributed to the water *(7, 17)*. From this FID, we obtain the Fourier-transformed NMR spectrum, which is as presented in the lower graph.

The experiment of Fig. 3 leads to several observations. First, it is possible to measure the ratio of water to cellulose. NMR software is available to assist. (We use a program called "STEFIT" as part of the software of SPINMASTER.) Second, because of the extreme difference in $T_2$ values, it is possible to perform relaxation measurements both for the water and for the cellulose component of the paper simply by choosing different time intervals *(18)*. Third, the sharpness of the water signal can be used to define a "freezing point" for the water, or a parameter that gives information on the nature of hydrogen bonds between the water and the cellulose *(17)*.

Moreover, the same method allows us to measure the molar ratio of cellulose to total water and that of cellulose to bound water. The ratio for total water can be obtained from the origin intercepts of the best fit curve that represents the full FID (insert in Fig. 3). To determine the ratio for bound water, we can apply the same method at a lower temperature (263 K). In this way, the bound water is measured by freezing the free water and measuring the signal of residual water. The same experiments might give information on porosity as a function of the temperature *(19)*.

The sharpness of the water signal can also be used as a tool for analysis in the NMR imaging of any paper-containing material, such as a book or a document *(20)*. A careful simulation of the FID experiments was performed on each sample, leading to the water/cellulose ratios shown in Table II. As the data show, the amount of water does not depend on the sizing. Instead, the ratio is a characteristic of the type of paper.

In ancient, well-preserved sheets of paper—paper of extreme high quality and made of rags—the amount of water is constant and identical to the amount observed in linters samples. This amount, including both free and bound water, corresponds to 0.9 molecules of water per glucose monomer. The amount of free water is almost negligible. In paper of inferior quality, the amount of total water is greater, which confirms that free water contributes to the total amount.

The $T_1$ measurements can be performed separately on cellulose signals and on water signals at room temperature. **Table III** lists data from measurements of the $T_1$ relaxation times attributed to the slow relaxation cellulose component. Remember, however, that for each type of paper, there are two $T_1$ components. One component can be attributed to domains poor in paramagnetic impurities, accounting for 85–90% of the total magnetization. The other component can be attributed to domains rich in paramagnetic impurities, which would account for 10–15% of the total magnetization. This assignment derives from the observation that the short component of $T_1$ relaxation times does not seem to be related to the type of paper nor to its sizing. In support of this observation, the data in **Fig. 4** show a lack of correlation between these fast relaxation components.

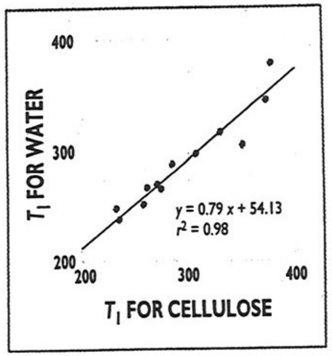

*5. Slow relaxing components of $T_1$ for water and $T_1$ for cellulose in the range of 243–298 K. Data are relative to the linters sample with neutral sizing.*

The short relaxing component is undoubtedly related to domains rich in paramagnetic impurities, and it is present in all samples. As previously shown, the presence of iron and other paramagnetic impurities is common to all our samples, as demonstrated by EPR spectra. These paramagnetic impurities are introduced in the manufacturing process. Consequently, the fast $T_1$ relaxing component related to paramagnetic impurities will be ignored in this context, and we will turn our attention to the slow $T_1$ relaxing component.

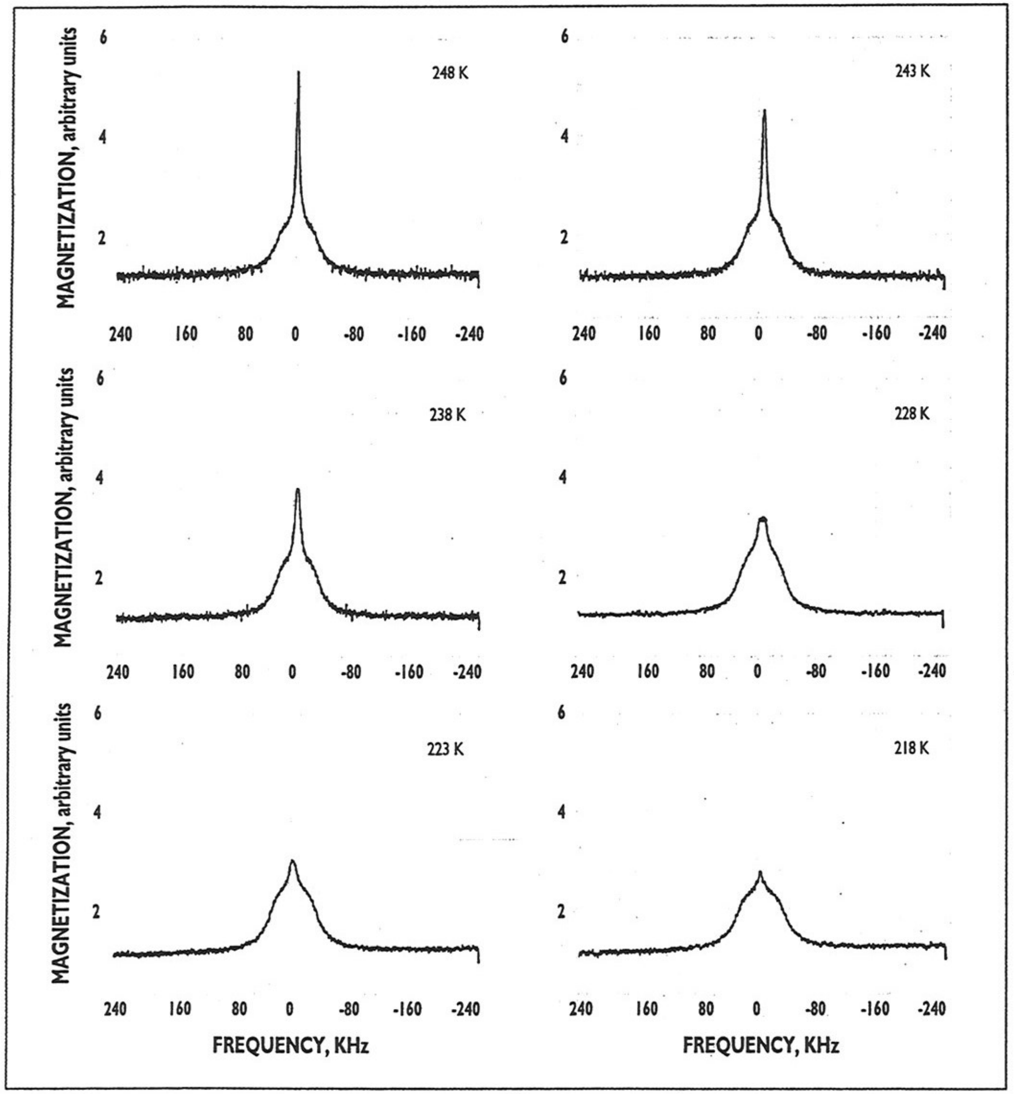

*6. ¹H NMR spectra of a groundwood paper with neutral sizing at different temperatures. The sharp line on top of the broad one is from bound water, which is highly mobile even at low temperatures.*

To characterize the nature of the water and the energies associated with the motions of water binding and the cellulose internal motions, we performed a full $T_1$ (spin-lattice) relaxation study as a function of the temperature. By this procedure, it is possible to quantify the amount of free and bound water *(21, 22)*.

In all paper *(7, 17)* and cotton samples, it is possible to measure the relaxation parameters of the cellulose simply by using the first few points of the magnetization measured in the time domain. Conversely, using points after at least 50 µs, we derive only the relaxation parameters relative to the water component.

This observation is true until the temperature decreases to about 243 K, where the water resonance broadens and progressively merges into the broad cellulose resonance. As **Fig. 5** indicates, the slow relaxing components of cellulose and water are strictly related by the spin diffusion process, which is still active at low temperatures.

Thus, even if the line width distinction ($T_2$) between the two components is present at a low temperature, as a result of spin diffusion, no $T_1$ distinction is observed. As **Fig. 6** shows, the water peak can be observed down to about 218 K.

Furthermore, the freezing point of bound water is much lower than

| | LINTERS | | KRAFT | | GROUNDWOOD | |
|---|---|---|---|---|---|---|
| Temp., K | Neutral | Acid | Neutral | Acid | Neutral | Acid |
| 298 | 349±10 | 293±20 | 244±8 | 250±11 | 143±4 | 96±6 |
| 293 | 354±10 | 273±20 | 203±5 | 242±12 | 135±7 | 98±6 |
| 288 | 329±7 | 277±15 | 196±4 | 226±13 | 132±3 | 98±7 |
| 283 | 307±8 | 250±10 | 185±6 | 205±8 | 126±3 | 98±5 |
| 278 | 284±7 | 240±7 | 178±3 | 183±4 | 121±4 | 95±7 |
| 273 | 274±5 | 234±8 | 183±8 | 179±4 | 130±4 | 98±6 |
| 268 | 261±8 | 231±6 | 182±8 | 165±5 | 164±6 | 108±13 |
| 263 | 233±11 | 240±9 | 199±5 | 168±5 | 161±4 | 112±8 |
| 258 | 241±8 | 236±7 | 228±7 | 183±7 | 190±5 | 129±8 |
| 253 | 235±11 | 290±14 | 261±4 | 220±6 | 235±5 | 151±9 |
| 248 | 270±8 | 355±30 | 286±7 | 278±6 | 297±5 | 182±11 |
| 243 | 376±7 | 533±40 | 407±9 | 394±10 | 374±9 | 225±13 |
| 238 | 513±16 | 787±50 | 606±15 | 528±18 | 434±10 | 334±21 |
| 233 | 714±18 | 1026±100 | 815±25 | 774±24 | 466±11 | 360±30 |
| 228 | 1040±31 | 1581±100 | 987±45 | 978±27 | 559±17 | 445±35 |
| 223 | 1510±40 | 2102±160 | 1401±68 | 1277±63 | 613±16 | 489±35 |
| 218 | 2260±90 | 2742±180 | 1744±80 | 1688±70 | 659±25 | 520±42 |
| 213 | 3000±140 | 3243±200 | 2553±110 | 1823±73 | 710±33 | 603±50 |
| 208 | 3430±150 | 3475±300 | 3202±130 | 2393±100 | 728±34 | 651±52 |
| 203 | 4590±250 | 3273±240 | 4109±250 | 3010±250 | 799±38 | 672±52 |
| 198 | 6290±350 | 4078±370 | 4498±288 | 3371±250 | 808±40 | 672±50 |
| 193 | 7260±400 | 4991±300 | 5108±320 | 4040±300 | 850±40 | 617±60 |
| 188 | 8100±500 | 5341±400 | 5787±400 | 4390±350 | 906±48 | 692±50 |
| 183 | 9770±600 | 6451±450 | 7134±500 | 4590±400 | 906±50 | 645±45 |

*III. $T_1$ spin–lattice relaxation times for the slow relaxing component of cellulose, milliseconds*

| Sample | Relative amount of water |
|---|---|
| Linters | |
| Neutral | 72 |
| Acidic | 69 |
| Kraft pulp | |
| Neutral | 88 |
| Acidic | 75 |
| Groundwood pulp | |
| Neutral | 100 |
| Acidic | 97 |
| Ancient paper | 68 |

Temperature of 298 K.
Less than 2% error.

*IV. Relative amount of water as measured with a conventional spectrometer*

| Sample | Activation energy, KJ/mole |
|---|---|
| Linters | |
| Neutral | 30.8±0.5 |
| Acidic | 29.0±0.8 |
| Kraft pulp | |
| Neutral | 26.9±0.9 |
| Acidic | 27.3±0.9 |
| Groundwood pulp | |
| Neutral | 22.0±1 |
| Acidic | 21.0±1 |

*V. Activation energies for the cellulose–water system*

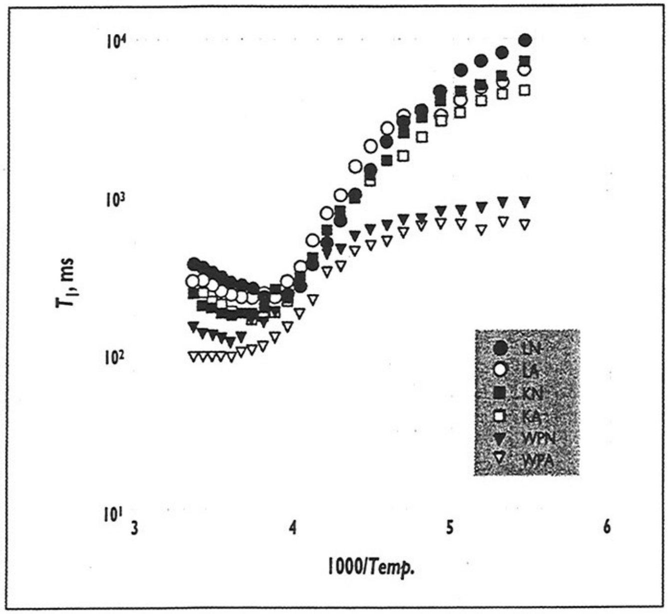

*7. Semilogarithmic plot of the long relaxing component of $T_1$ for cellulose vs. 1000/Temp. for all paper samples. $T_1$ relaxation times are quite distinctive, especially at low temperatures.*

273 K *(23)*. In particular, we can define different types of water in which the freezing point differs according to the type of hydrogen bonds and cellulose packing *(5, 24)*. Different cellulose polymorphs and hemicelluloses are differently packed, and they contain different amounts of bound water, according to data reported previously *(1, 3, 4, 7)*.

To clarify this point, we quantitatively analyzed bound water as a function of the temperature. We checked these results by using a different method to measure the relative amount of total water. This measurement was made with a high-resolution conventional spectrometer at 200.13 MHz. The data are listed in **Table IV**. The area has been set to 100 in the case of the neutral groundwood pulp sample, and all other integrals have been normalized with respect to this sample. The relative amount of water measured at 57.0 MHz was found to be in good agreement with the relative amount of water measured at 200.13 MHz.

The most significant independent parameter that can be obtained from relaxometric measurements is the activation energy, as related to overall motions (segmental motions plus rotations) of the cellulose-water system. In fact, the bulk magnetic response and the motions of magnetic moments are correlated with the onset of molecular motions, which in turn are responsible for mechanical and dielectric losses *(25)*. Thus, the measurement of $T_1$ as a function of the temperature can be used to give indications on the local stiffness and on correlation times associated with local motions *(17)*. Data of this type are quite common in synthetic polymer physics, but these types of analysis have not been attempted on paper samples. The results of a careful $T_1$ relaxation study on the cellulose signal as a function of the temperature are presented in Table III and **Fig.** 7.

In the low temperature range of 248–203 K, at the right side of the $T_1$ minimum where $\omega_0 \tau_0 \approx 1$, log $T_1$ is linearly dependent on 1000/*Temp.* (Fig. 7). From this relationship, it is easy to obtain the activation energies for the overall motions of the cellulose–water system. The overall motion consists of segmental motions, rotations for the cellulose, and translations plus rotations for the water component. These values are listed in **Table V.**

One conclusion that emerges from the temperature dependence of $T_1$ relaxation for different samples is that all curves are distinct and separate. In particular, by comparing data for neutral or acidic sizing for each type of paper, we see that the acid sizing shortens $T_1$ relaxation times in the low temperature range, as Fig. 7 illustrates. At low temperatures, relaxation times are slightly shorter for all papers with sizing, with respect to their neutral counterparts. This slight decrease is probably caused by paramagnetic impurities contained in the acid sizing (rhombic Fe).

The energies presented in Table V are the Arrhenius activation energies for the overall motion of the cellulose–water system. In this system, many motions can contribute to the overall relaxation. If we think of cellulose as a polymer in which the overall chain motion is dominated by the rotations around the glycosidic bonds, we can reasonably assume that the higher the overall energy, the higher will be the order (crystalline content) and the orientation of macromolecules in cellulose fibers.

Besides the activation energy of cellulose, the other factor that contributes to the overall motion pertains to the water, which is in spin diffusion with the cellulose. Again, a high activation energy of the water means a water with a tight bond to the cellulose. A lower energy means a loosely bound water molecule, such as a micro-drop of free water confined in a micro-hole.

Thus, the higher the overall activation energy, the higher the "quality" of the paper should be. This parameter is exactly the "cold" parameter needed to define both the physical quality of a paper sheet and its eventual degradation state after artificial aging or external contamination. Here the term "high quality" is used in a strictly physical context. The term pertains to a paper sheet with cellulose as crystalline as possible and water as tightly bound as possible.

**KEYWORDS**

*Activation energy, bibliographies, bound water, cellulose, degradation, electron spin resonance, free water, nuclear magnetic resonance, paper, relaxation.*

### CONCLUSION

Paper can be thought of as a two-component material, made mostly of cellulose and water. This view is particularly useful in analytical studies carried out with proton NMR techniques. In this way, the nature and quantity of bound water can be substantially clarified. The effect of a particular sizing, for example, can be observed.

In the system of cellulose-bound water, the overall activation energies correlate well with the intrinsic merit of the paper ($E_{\text{linters}} >> E_{\text{kraft}} >> E_{\text{groundwood}}$). This measurement can be considered together with the total amount of bound water and the total amount of free water to define a quality factor. This quality factor might be used in identifying criteria for the study of paper of different origins and for the study of artificial aging of paper. **TJ**

---

*Capitani is researcher and Segre is research director at Istituto di Strutturistica Chimica and NMR Service, CNR, Area della Ricerca, MB10, 00016 Monterotondo Staz. Rome (Italy). Attanasio is first researcher at Ist. di Chimica dei Materiali MB10, 00016 Monterotondo Staz. Rome(Italy). Blicharska is dozent at the Dept. of Physics, Yagellonian Univ., ul. Reymonta, Kracow (Poland). Focher and Capretti are director and researcher, respectively at Staz. Sperimentale Cellulosa e Carta, Pza. L. da Vinci 20133 Milano (Italy).*

*This work has been partly supported by a special ad hoc program "Technology applied to Cultural Heritage." The authors are grateful to A. Guarino for the continuous support and helpful discussions.*

*Received for review April 26, 1995.*

*Accepted Sept. 22, 1995.*

## LITERATURE CITED

1. Earl, W. L. and VanderHart, D. L., *Macromolecules* 14: 570(1981).
2. MacKay, A. L., Bloom, M., Tepfer, M., *et al., Biopolymers* 21: 1522(1982).
3. Atalla, R. H. and VanderHart, D. L., *Science* 223: 283(1984).
4. VanderHart, D. L. and Atalla, R. H., *Macromolecules* 17: 1465(1984).
5. Sugiyama, J., Vuong, R., and Chanzy, H., *Macromolecules* 24: 4168(1991).
6. Horii, F., Hirai, A., and Kitamaru, R., *Macromolecules* 20: 2117(1987).
7. Paci, M., Federici, C., Capitani, D., Perenze, N., *et al., Carbohydrate Polymers*, 26:289(1995).
8. MacKay, A. L., Tepfer, M., Taylor, I. P., *et al., Macromolecules* 18: 1124(1985).
9. Attanasio, D., Capitani, D., Federici, C., *et al.*, in *Multidimensional Spectroscopy of Polymers: Vibrational, NMR, and Fluorescence Techniques* (M. Urban and T. Prouder), ACS Symposium Series #598, American Chemical Society, Washington, DC, 1995, Ch. 19.
10. Attanasio, D., Capitani, D., Federici, C., *et al., Archaeometry* 37: 377(1995).
11. Cotton, S. A. and Gibson, J. F., *J. Chem. Soc. A* 1696(1971).
12. Farrar, T. C. and Becker, E. D., *Pulse and Fourier Transform NMR*, Academic Press, London 1971.
13. Fukushima, E. and Roeder, S. B. W., *Experimental Pulse NMR. A nuts and bolts approach*, Addision-Wesley, Reading, MA, 1981.
14. Press, W. H., Teukolsky, S. A., Flammery, B. P., *et al., Numerical Recipes. The Art of Scientific Computer*, Cambridge University Press, Cambridge, England, 1988.
15. Barclay, L. R. C., Cromwell, G. R., and Hilborn, J. W., *Canad. J. Chemistry* 72: 35(1994).
16. Gibson, J. F., in *ESR and NMR of Paramagnetic Species in Biological and Related Systems* (I. Bertini and R. S. Drago, Eds.), D. Reidel Publ. Co., Dordrecht, 1980, Ch. 10.
17. McBrierty, V. J. and Packer, K. J., *Nuclear Magnetic Resonance in Solid Polymers*, Cambridge University Press, Cambridge, England, 1993.
18. Segre, A. L., Capitani, D., Fiordiponti, P., *et al., Europ. Polym. J.* 28: 1165(1992).
19. Strange, J. H. and Rahaman, M., *Phys. Rev. Lett.* 71: 3589(1993).
20. Segre, A. L., Capitani, D., Malinconico, M., *et al., Material Sci. Lett.* 12: 728(1993).
21. Quinn, F. X., Kampff, E., Smyth, G., *et al., Macromolecules* 21: 3191(1988).
22. Smyth, G., Quinn, F. X., and McBrierty, V. J., *Macromolecules* 21: 3198(1988).
23. Blicharska, B., Florkowski, Z., Hennel, J. W., *et al., Biochim. Biophys. Acta* 207: 381(1970).
24. Isogai, A., Usuda, M., Kato, T., *et al., Macromolecules* 22: 3168(1989).
25. Connor, T. M., *Trans. Farad. Soc.* 60: 1574(1963).